# Supplementary Information

## Visible Light Responsive ZnCuO Nanoparticles: Benign Photodynamic killers of Infectious Protozoan

*Akhtar Nadhman*, Samina Nazir*, Malik Ihsanullah Khan, Attiya Ayub, Bakhtiar Muhammad, Momin Khan, Dilawar Farhan Shams, Masoom Yasinzai*

### Characterization of synthesized nanostructures

#### *XRD analysis*

X-rays diffraction measurement was performed on a diffractometer (Shimadzo 6000) equipped with Cu Kα1 (λ=1.5406 nm) at a voltage of 40 kV and a current of 30 mA. The observed diffraction peaks in the recorded XRD pattern agreed well for the hexagonal ZnO having wurtzite structure.[1] No characteristics peaks of other impurities were observed in XRD pattern, indicating that phase-pure and high quality ZnO nanomaterials were readily obtained (Figure S1). The main diffraction peaks were indexed to wurtzite ZnO (hexagonal) appeared at 2θ =31.6°, 34.5°, 36.3°, 47.6°, 56.6°, 62.9°, 66.6°, 68.0° and 69.2°. Average crystalline sizes of all synthesized samples were calculated by using Scherrer's formula[2] by averaging results from all the crystallographic peaks.

Average crystalline size (D) = $k\lambda/\beta\cos\theta$ (1)

Where, λ is wavelength (1.54A°), β is FWHM (full width half maximum) and θ is the Bragg's diffraction angle. Thus, the obtained values were 16-24nm (Table S1) and it was also found in the TEM results (Figure S2).

It can be elucidated from Figure S1 that a steady decrease in the peak intensity was noted with increasing amount of Cu (from ZnCuO1 to ZnCuO2). Additionally, Cu did not result any additional peaks corresponding to Cu related secondary or impurity phase. Moreover, no remarkable shift of diffraction peaks were observed among pure or non-doped ZnO (ndZnO) and ZnCuO particles, which revealed that the lattice expansion or shrinkage should be neglected. It might be therefore inferred that Cu was incorporated into the Zn lattice in the standard wurtzite structure in ZnCuO1 and ZnCuO2, rather at the interstitial sites that occupied substitution site in the ZnO lattice. However, in case of ZnCuO3, Cu was incorporated into the interstitial site that resulted in increase of peak intensity. While in case of ZnCuO4, doped nitrogen into the crystal lattice of ZnO did not bring a new object phase. However, a significant shift in 2θ was observed, which indicated that by nitrogen doping, nitrogen occupied the oxygen vacancy and did not replace the Zn atom from the lattice sides. In ZnCuO4, it occupied the substitution and then went to interstitial and again came back to substitution with an increase in concentration that resulted a considerable shift in the peak position.

Further, Figure S3 signifies a clear pattern of the three main peaks and it was observed that the peak intensity was increased by the addition of Cu concentration and hence, the $Cu^{2+}$ ions were understood to have occupied the Zn without changing the crystal structure. It was evident that orientation behavior of ZnO was strongly promoted by Cu-doping.[3]

(a)

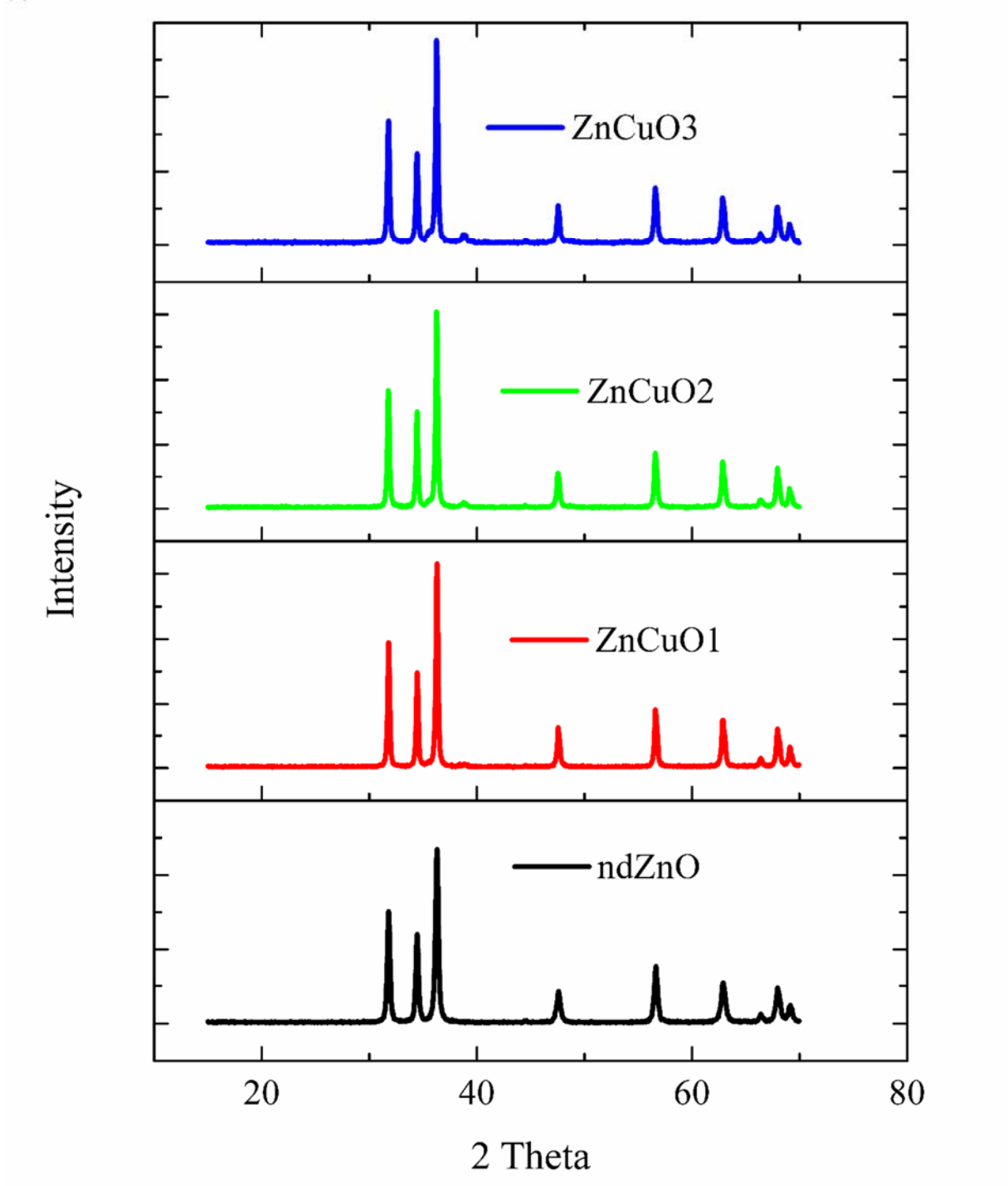

(b)

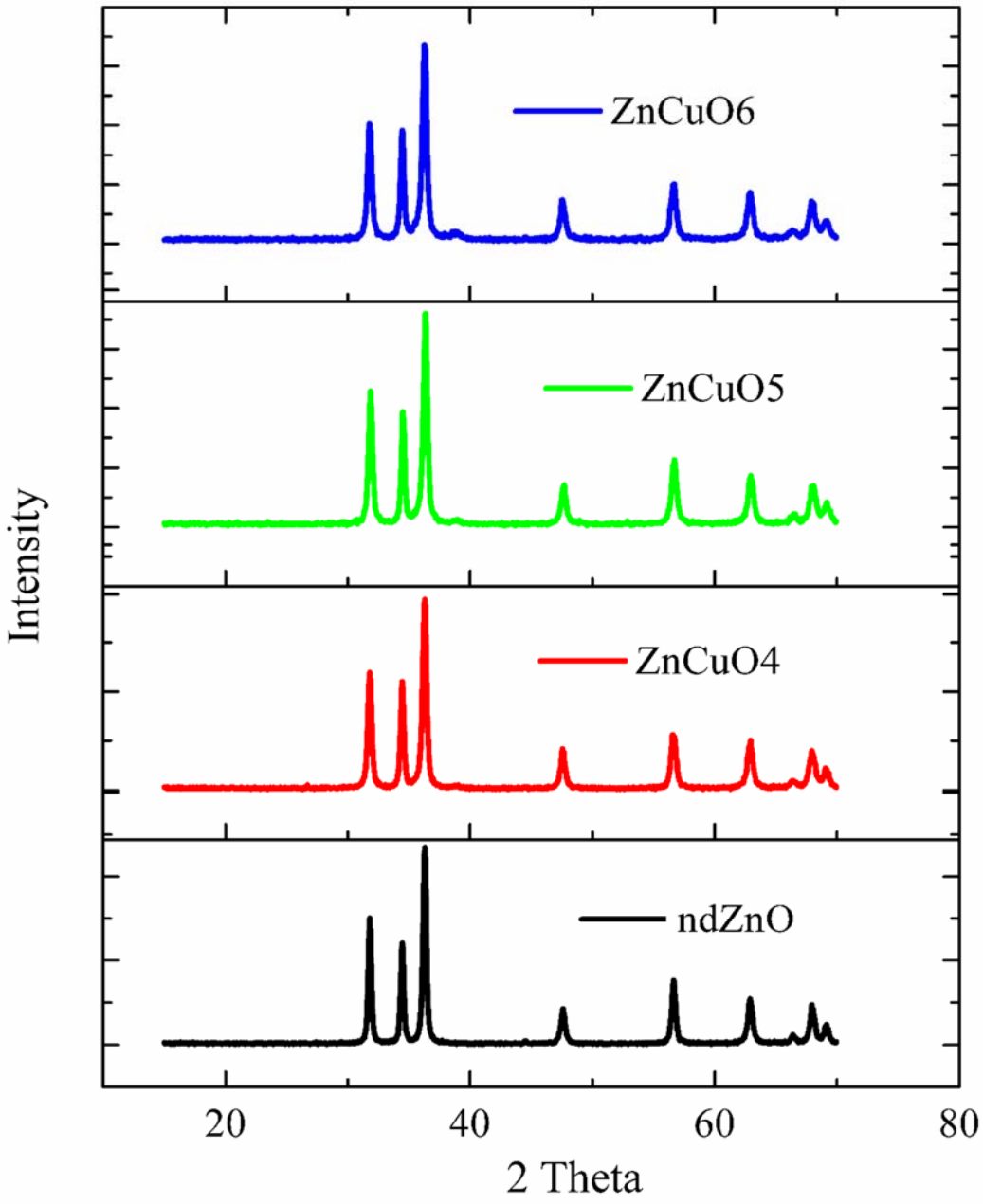


Figure S1 XRD patterns of ZnO, Cu & Cu/N doped ZnO nanostructures having 1, 5 and 10% ratio.

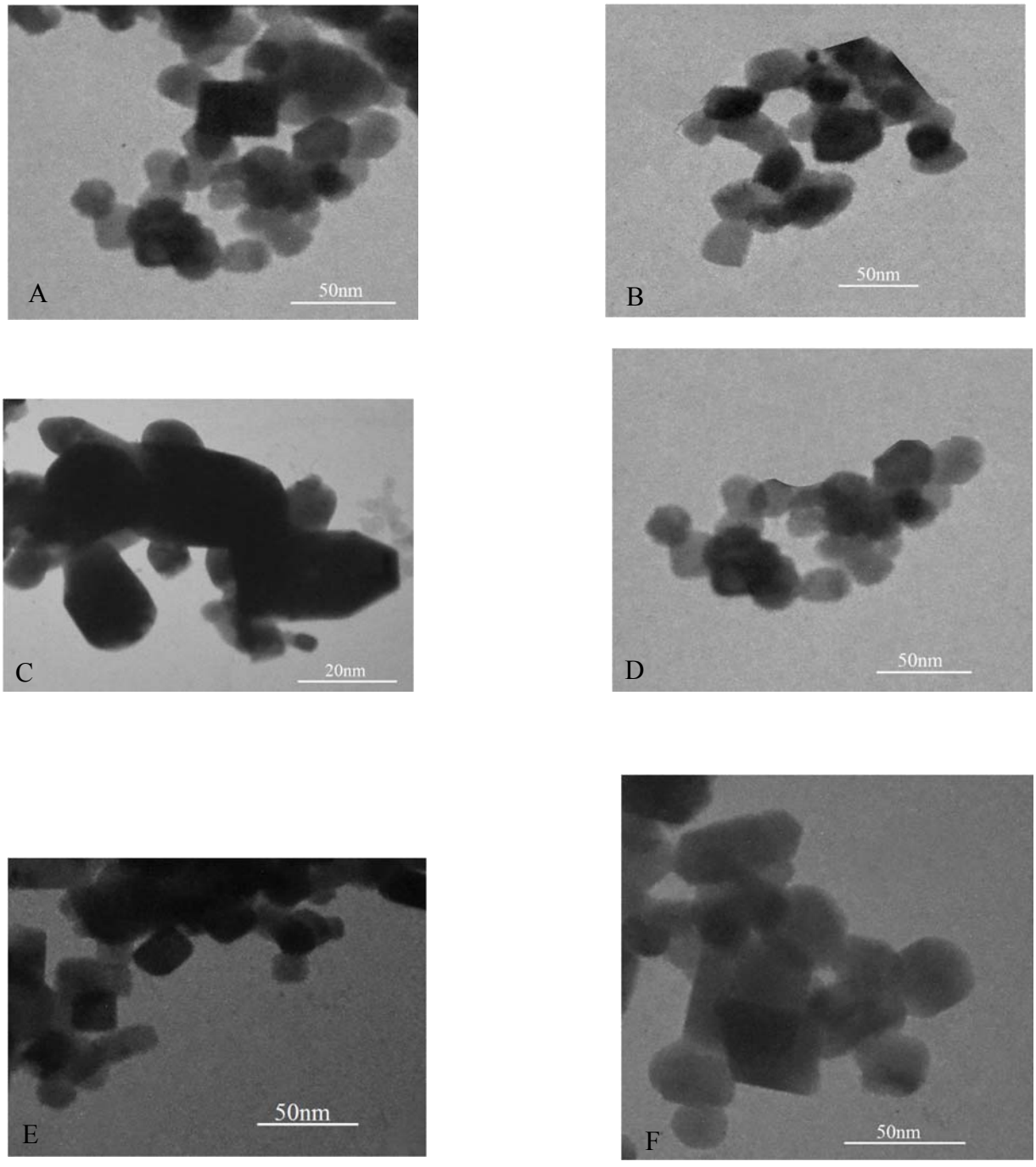


Figure S2 TEM images of ZnCuO nanoparticles (20-100nm).

Note: (a) ndZnO (b) ZnCuO1 (c) and (d) ZnCuO3 (e) ZnCuO4 (f) ZnCuO6.

(a)

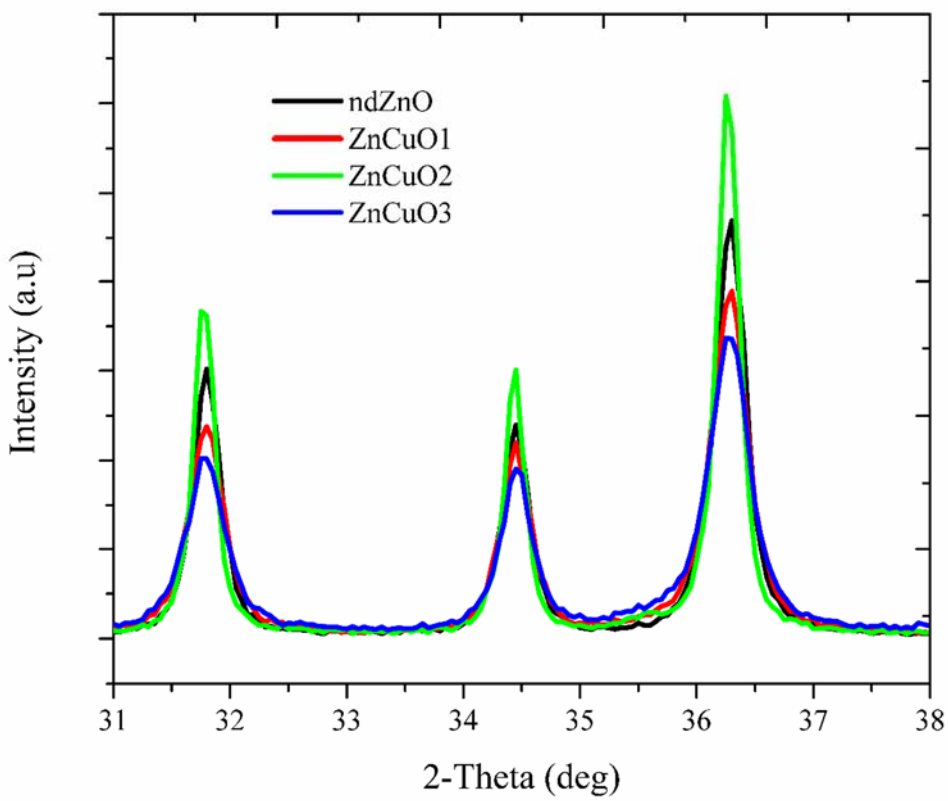


(b)

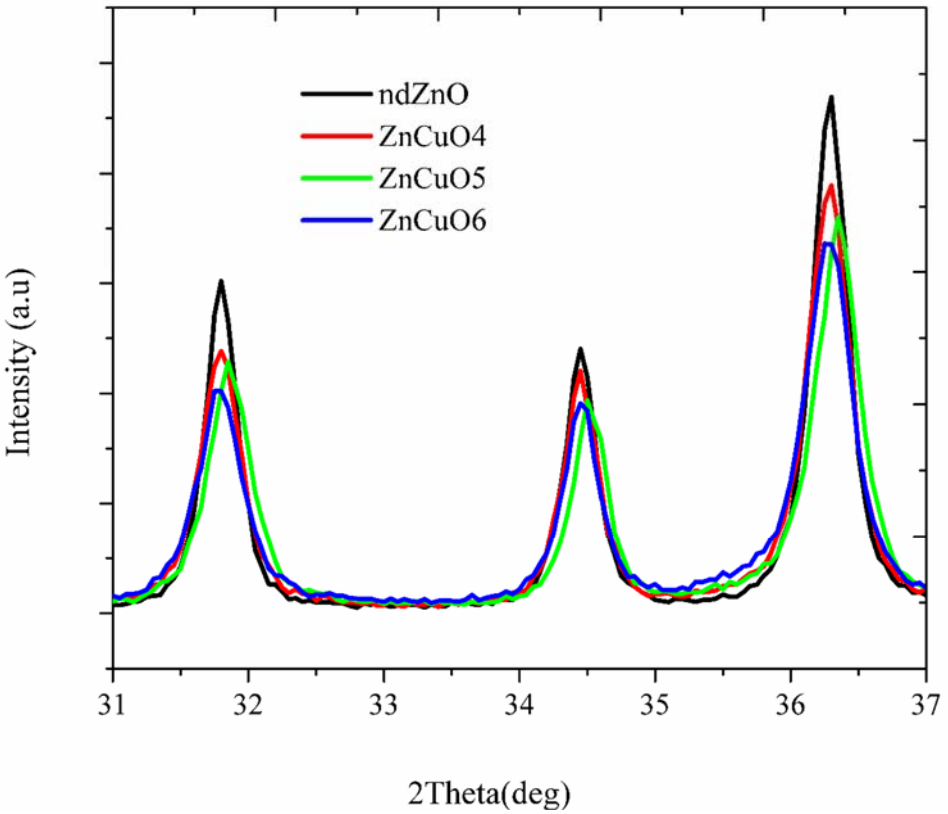


Figure S3 Clear pattern of main peaks of ZnCuO nanoparticles and ndZnO on XRD.

Table S1 Average crystalline size of the nanoparticles calculated by Scherrer's equation

| **Samples** | **Cell parameter (Å)** | | **c/a Ratio** | **unit cell** | **Microstrain = βCosθ/4** | **Crystalline Size D=kλ/βcosθ** |
|---|---|---|---|---|---|---|
| Nanocrystals | a=b | C | | volume | $(\varepsilon)(10^{-3})$ | (nm) |
| ndZnO | 3.2503 | 5.2075 | 1.6021 | 47.6424 | 0.12845 | 24 |
| ZnO: CuO (1%) | 3.2521 | 5.2193 | 1.6049 | 47.8033 | 0.15747 | 16 |
| ZnO: CuO (5%) | 3.2556 | 5.2196 | 1.6032 | 47.9090 | 0.16164 | 17 |
| ZnO:CuO(10%) | 3.2578 | 5.2098 | 1.5991 | 47.8837 | 0.16581 | 21 |
| ZnO:CuO:N(1%) | 3.2541 | 5.2095 | 1.6009 | 47.7722 | 0.14919 | 20 |
| ZnO:CuO:N(5%) | 3.2557 | 5.2105 | 1.6004 | 47.8284 | 0.16161 | 18 |
| ZnO:CuO:N(10%) | 3.2558 | 5.2117 | 1.6007 | 47.8423 | 0.16577 | 19 |

Diffuse reflectance spectroscopic (DRS) analysis

Perkin Elmer UV/VIS/NIR spectrometer-lambda 950, with integrating sphere ranges between 900nm to 2500nm was used to check the optical properties of prepared samples. In Figure S4, DRS spectrum of ndZnO showed a small peak below 400nm that was the absorption in UV region. While ZnCuO1 to ZnCuO3 showed characteristic absorption edge near 430-455nm related to oxygen defects and indicating visible region of the spectrum. The ndZnO line from figure S4 (a) has not been added because of the overlapping of the ZnCuO1 with ndZnO.

It is evident in Figure S4 that ndZnO showed a strong absorption edge at 450nm which was related to oxygen defects.[4] ZnCuO nanostructures also showed small peaks related to oxygen defects appeared at 450nm except ZnCuO1. However, in case of ZnCuO4 to ZnCuO6, the increasing dopant concentration decreased the visible response (Figure S4b). Moreover, ZnCuO1 showed strong absorption in visible region at 520nm while ZnCuO2 to ZnCuO3 showed a relatively weak absorption at 510-515nm.

(a)

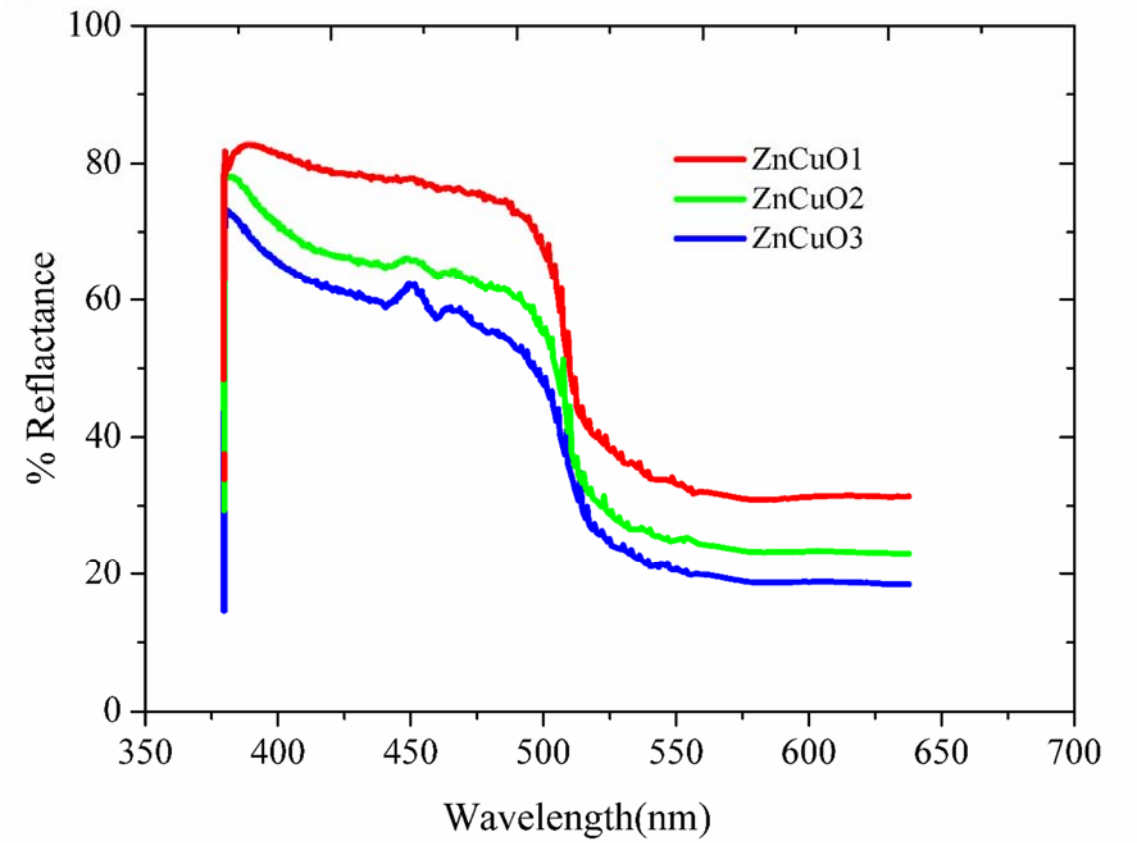


(b)

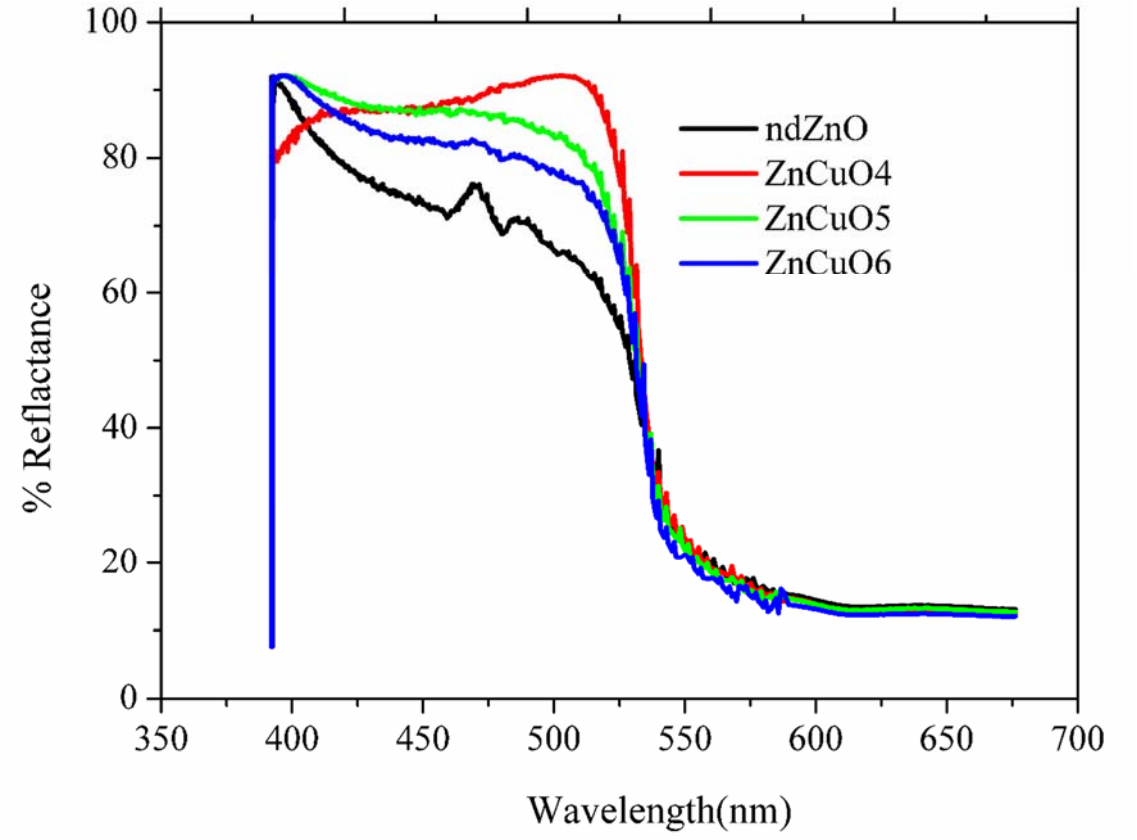


Figure S4 Diffuse reflectance spectra of ndZnO and ZnCuO nanoparticles.

***Band gap measurements***

DRS technique was also used to measure the optical band gap energies of all synthesized samples. Kubelka-Munk function[5] was used to calculate the band gap energies of all synthesized nanostructures;

$$F(R) = [F(R_\infty)\, hv]^{1/2} \quad (2)$$

Where;

F(R) is the Kubelka-Munk function, R represents the absolute value of reflectance and hv is the energy. Figure S5, represents the band gap energies of the ndZnO and ZnCuO1 to ZnCuO6, derived by plotting the square root of the Kubelka-Munk function $F(R)^{1/2}$ vs energy in electron volts (eV). The direct band gap energies of all synthesized samples were estimated from the intercept of tangents drawn to the plots shown in Figure S5.

More copper doping decreases band-gap

A drastic change in the band gap was observed with a change in the concentration from ZnCuO1 to ZnCuO6. However, the band gap of ndZnO was 3.0eV but by doping with Cu or nitrogen it shifted to 2.6-2.9eV, which resulted a change in properties of the material. The decrease in the band gap energy with the addition of Cu can be attributed to structural interruption in the ZnO framework by Cu atoms resulting in smaller energy gap between the valence band and conduction band, the same happened with the Cu and nitrogen co-doped ZnO nanoparticles.[6] However, for the higher concentrations of Cu, nitrogen doping resulted in the slightly decreased band gap due to removal of some of Cu to interstitial sites as evident from lattice expansion already described in XRD results.

(a)

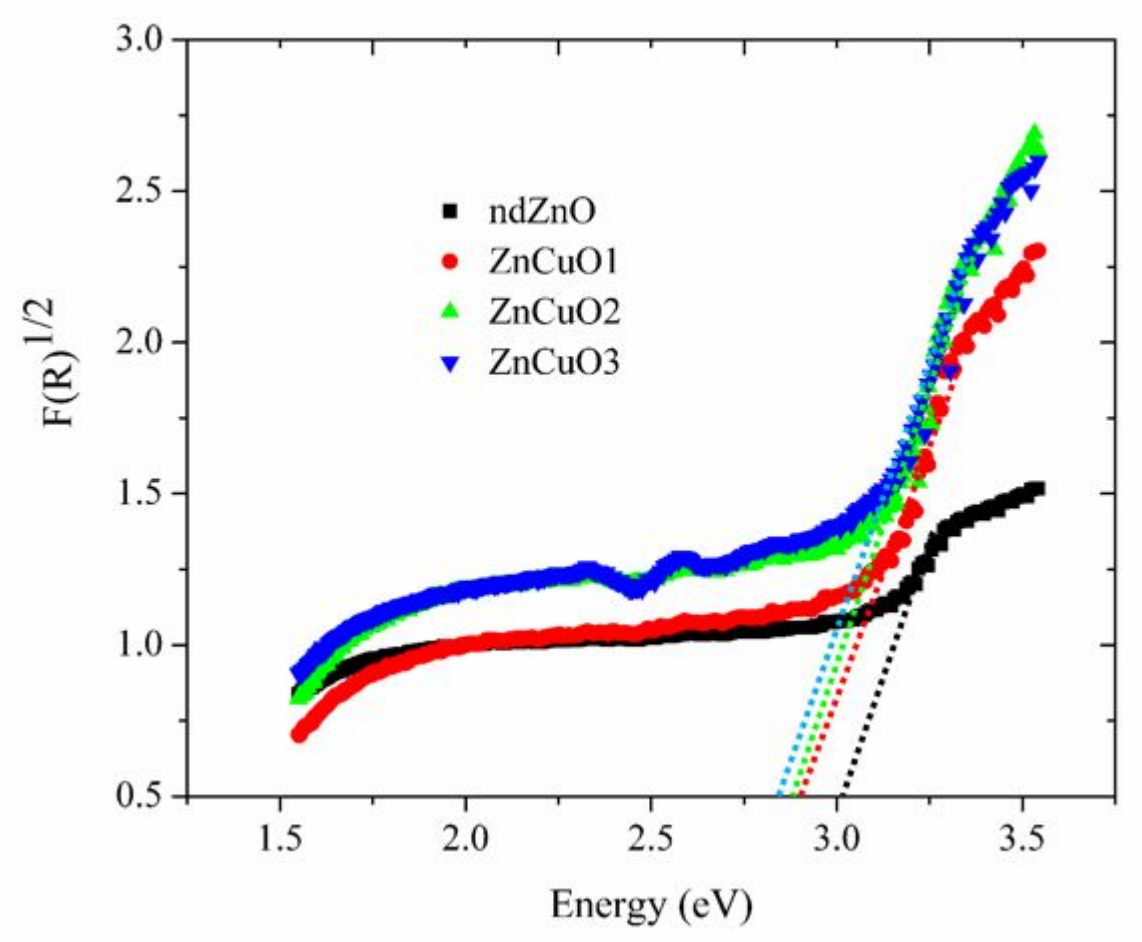

(b)

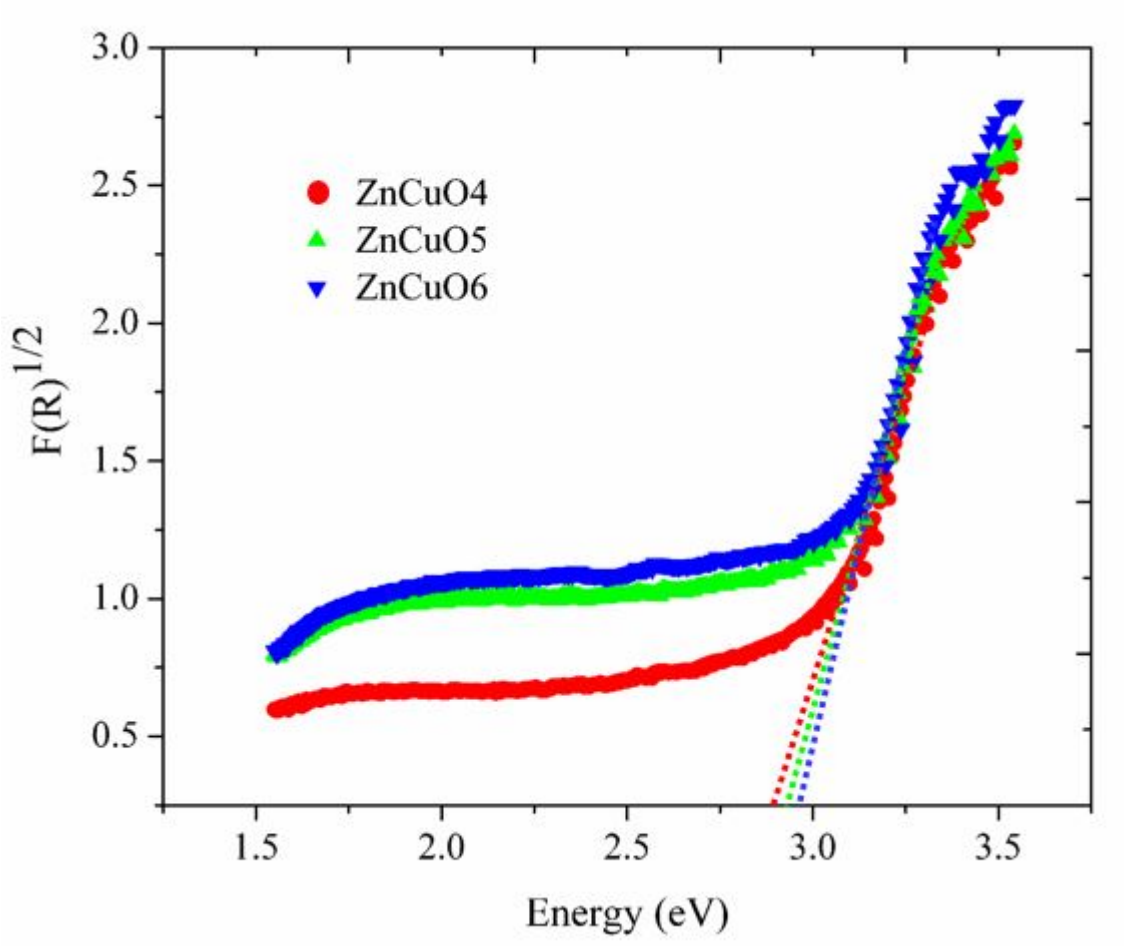


Figure S5 Band gap energies of ndZnO and ZnCuO nanoparticles, calculated by using Kubelka-Munk function.

***Photoluminescence (PL)***

Perkin Elmer photoluminescence LS 55 was used to verify the PL spectra of the synthesized samples at room temperature. Generally, the optical properties of metal oxide nanostructures were significantly affected by the densities of defects and oxygen vacancies. The PL spectra was used to investigate correlation between structure and property (Figure S6). It was noticed that there was a clear difference in the luminescence intensity of ndZnO and ZnCuO nanoparticles. The luminescence intensity of ndZnO was low as compared to that of ZnCuO nanostructures.[7] The PL spectra of ndZnO and ZnCuO1 to ZnCuO6 showed two distinct peaks on the wavelength scale. First emission peak was observed near 400nm in all samples while second peak was observed near 640-680 nm only in the Cu containing samples. ndZnO exhibited a very strong peak around 385-400nm related with UV-Vis response, which can be attributed to recombination of excitons corresponding to band edge emission of ZnO. However, a very minute peak in the visible region was observed at 736 nm in ndZnO corresponding to some oxygen deficiency.
The results obtained from PL were closely related to that of DRS. Peak at 400 nm for the ZnCuO nanoparticles corresponded to the band edge emission in all these structures. The emission peak at 640-680nm in the PL spectra for the ZnCuO1 to ZnCuO6 corresponded to the red emission. In case of ZnCuO4 to ZnCuO6 nanoparticles (Figure S6b), a decrease in peaks intensity was observed with increase in Cu concentration. The visible emission band around 640-680nm was due to transition of a photogenerated electron from the conduction band to a deeply trapped hole[8] and the probable candidate for the trapping of

holes are $O^{-2}/O^{-}$ ion at the surface. With the increase of nitrogen as dopant, a decrease in $O^{-2}/O^{-}$ surface ions led to a decreasing PL intensity for the red emission peak in ZnCuO4-6 structures.

(a)

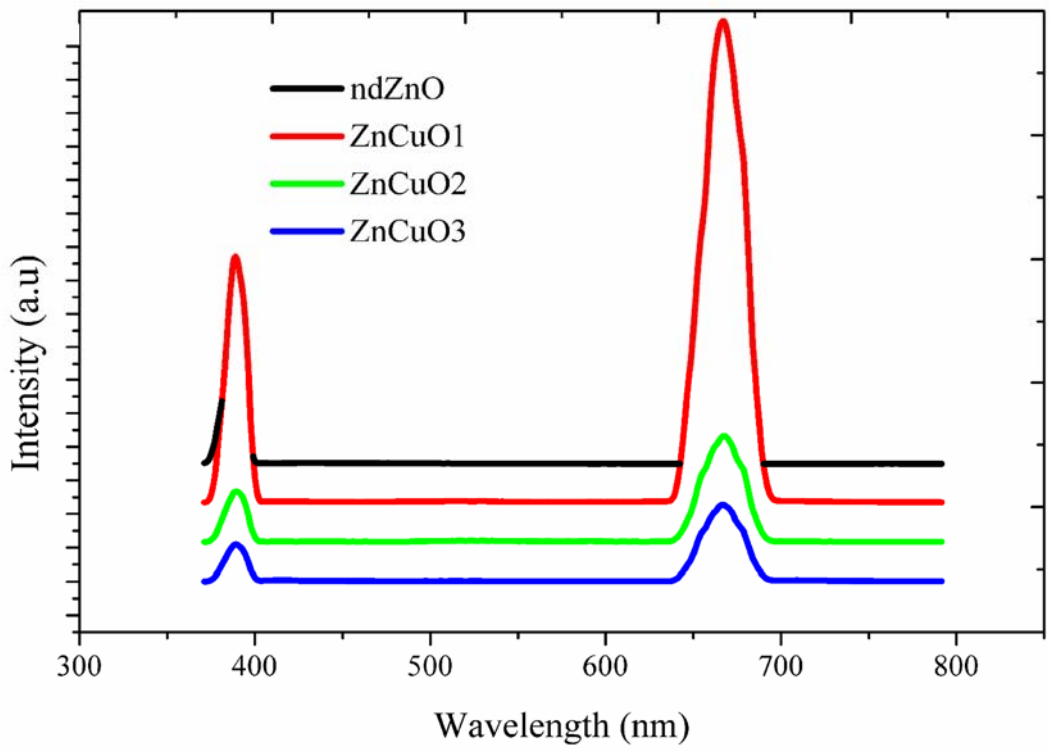


(b)

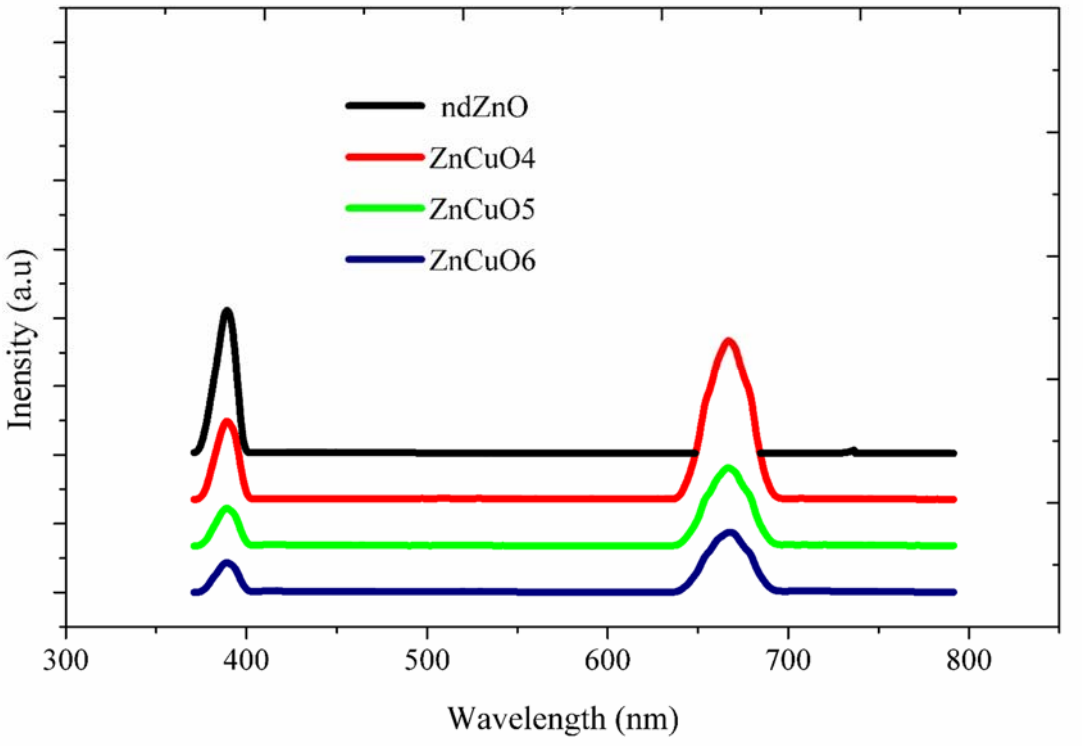


Figure S6 Photoluminescence spectra of ndZnO and ZnCuO nanoparticles.

**Rutherford backscattering (RBS)**

Rutherford backscattering of both the ndZnO and ZnCuO nanoparticles before PEGylation (Figure S7). RBS was used to characterize defect densities, thickness and structures in the near surface region. Further, the spectra represents the purity of each synthesized nanoparticle.

(a)

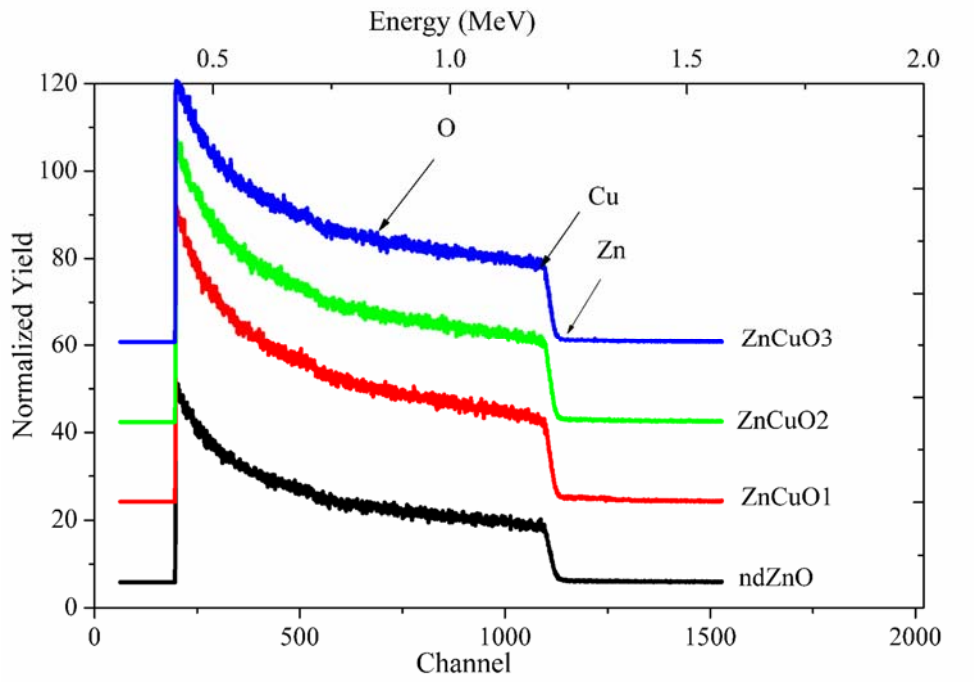


(b)

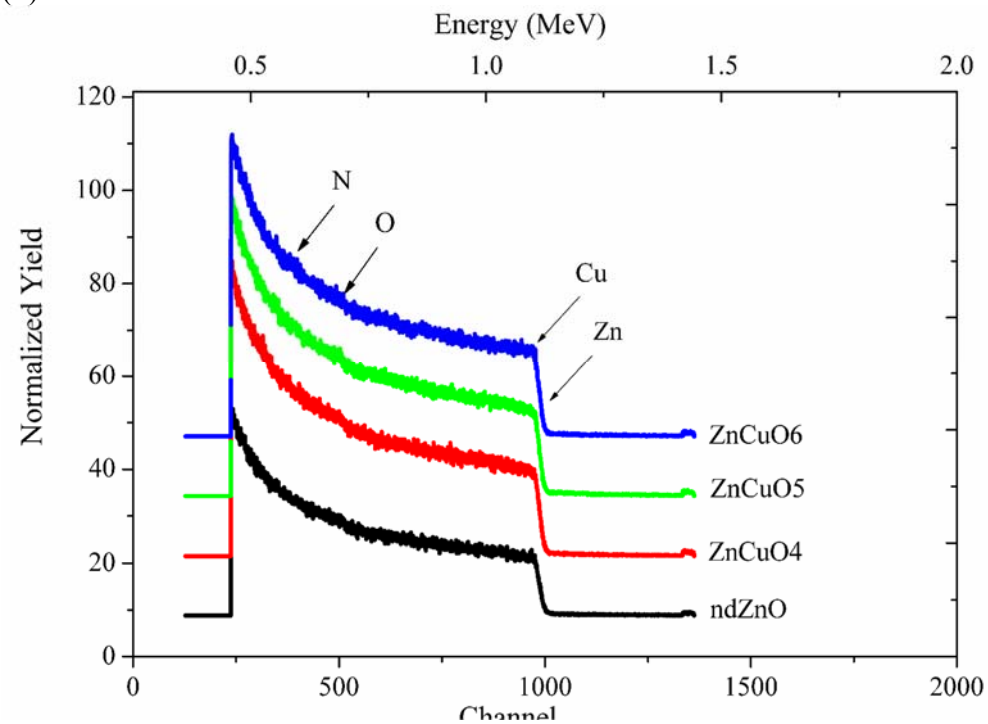


Figure S7 RBS of ndZnO and ZnCuO nanoparticles.

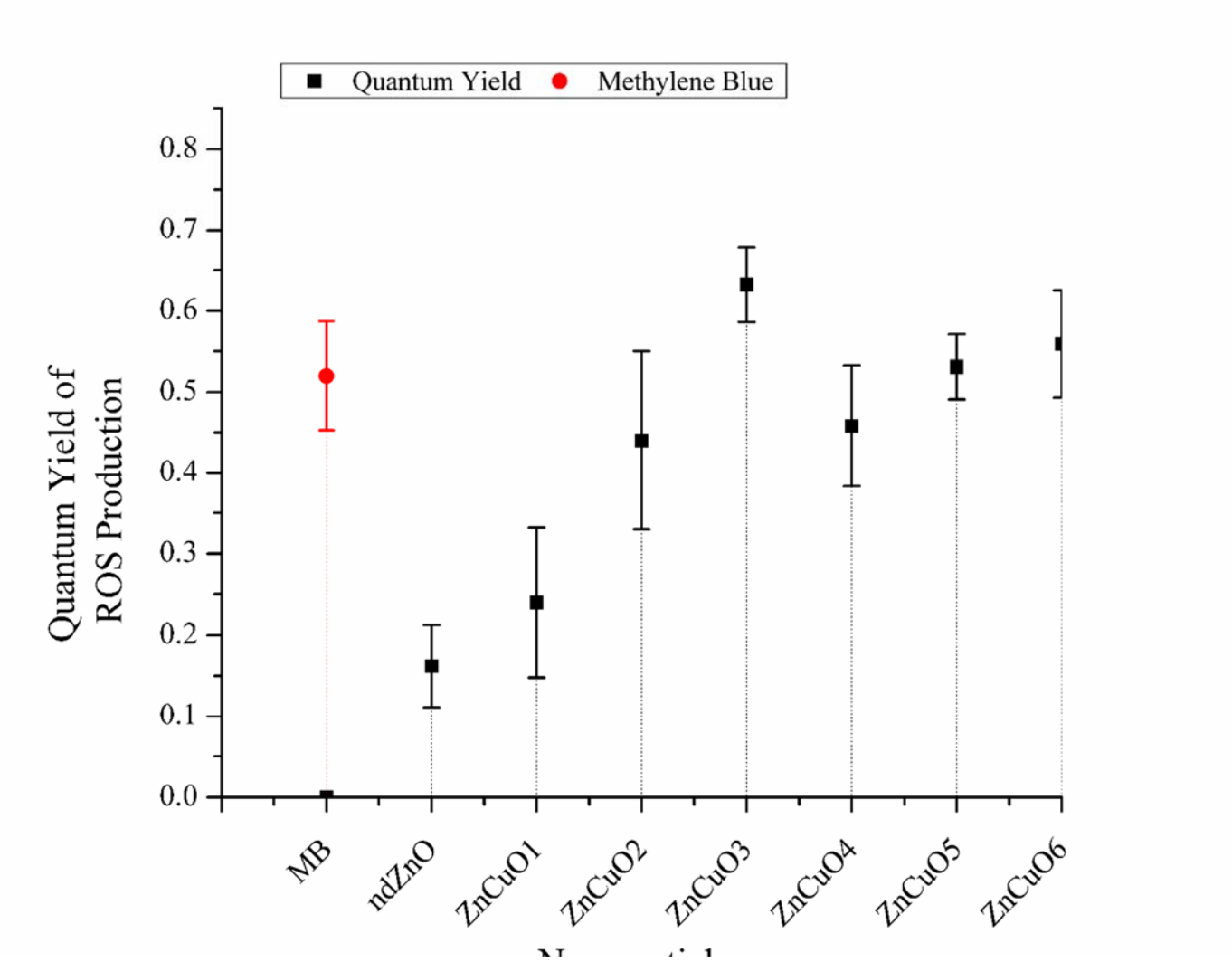


Figure S8 Quantum yield of ROS produced by ndZnO and ZnCuO nanoparticles. A clear statistical difference among ndZnO and ZnCuO nanoparticles ($p<0.05$). Red bar showing the ROS production by methylene blue (MB).

## REFERENCES


**1.** Muthukumaran S, Gopalakrishnan R. Structural, FTIR and photoluminescence studies of Cu doped ZnO nanopowders by co-precipitation method. *Optical Materials.* 2012;34(11):1946-1953.

**2.** Singhal S, Kaur J, Namgyal T, Sharma R. Cu-doped ZnO nanoparticles: Synthesis, structural and electrical properties. *Physica B: Condensed Matter.* 2012;407(8):1223-1226.

**3.** Chauhan R, Kumar A, Chaudhary RP. Synthesis and characterization of copper doped ZnO nanoparticles. *Journal of Chemical and Pharmaceutical Research.* 2010;2(4):178.

**4.** Qiu X, Burda C. Chemically synthesized nitrogen-doped metal oxide nanoparticles. *Chem. Phys.* 2007;339(1):1-10.

**5.** Mukhtar M, Munisa L, Saleh R. Co-precipitation synthesis and characterization of nanocrystalline zinc oxide particles doped with $Cu^{2+}$ ions. *Materials Sciences and Applications.* 2012;3:543.

**6.** Kim Y-S, Park C. Rich variety of defects in ZnO via an attractive interaction between O vacancies and Zn interstitials: origin of n-type doping. *Phys. Rev. Lett.* 2009;102(8):086403.

**7.** Elilarassi R, Sambasiva Rao P, Chandrasekaran G. Diluted magnetic semiconductor properties in Zn1−xCuxO nanoparticles synthesized by sol gel route. *J. Sol-Gel Sci. Technol.* 2011/01/01 2011;57(1):101-108.

**8.** Meyer B, Alves H, Hofmann D, et al. Bound exciton and donor–acceptor pair recombinations in ZnO. *Physica Status Solidi (b).* 2004;241(2):231-260.